Article type : Articles

Running Head: Evolution drives tissue stoichiometry

Title: Evolutionary history drives aspects of stoichiometric niche variation and functional effects within a guild

Authors: Carla L. Atkinson[a*], Brian C. van Ee[a], and J. Pfeiffer[b]

[a]Dept. of Biological Sciences, University of Alabama, Tuscaloosa, Alabama 35487, USA

[b]National Museum of Natural History, Smithsonian Institution, Washington, DC, USA

*Corresponding Author: Carla L. Atkinson, Address: Dept. of Biological Sciences, University of Alabama, Tuscaloosa, Alabama 35487, USA; Phone: +1-205-348-6805; Email: clatkinson@ua.edu

Abstract

Functional traits are characteristics of an organism that represent how it interacts with its environment and can influence the structure and function of ecosystems. Ecological stoichiometry provides a framework to understand ecosystem structure and function by modeling the coupled flow of elements (e.g. carbon [C], nitrogen [N], phosphorus [P]) between consumers and their environment. Animals tend to be homeostatic in their nutrient requirements and preferentially sequester the element in shortest supply relative to demand, and release relatively more of the element in excess. Tissue stoichiometry is an important functional trait that allows for predictions among the elemental composition of animals, their diet, and their waste products, with important effects on the cycling and availability of nutrients in ecosystems. Here we examined the tissue stoichiometric niches (C:N:P) and nutrient recycling stoichiometries (N:P) of several filter-feeding freshwater mussels in the subfamily Ambleminae. Despite occupying the same functional-feeding group and being restricted to a single subfamily-level radiation, we found that species occupied distinct stoichiometric niches and that these niches varied, in part, as a function of their evolutionary history. The relationship between phylogenetic divergence and functional divergence suggests that evolutionary processes may be shaping niche complementarity and resource partitioning. Tissue and excretion stoichiometry were negatively correlated as predicted by stoichiometric theory. When scaled to the community, higher species richness and phylogenetic diversity resulted in greater functional evenness and reduced functional dispersion. Filter-feeding bivalves are an ecologically important guild in freshwater ecosystems globally, and our study provides a more nuanced view of the stoichiometric niches and ecological functions performed by this phylogenetically and ecologically diverse assemblage.

Key Words: functional diversity, nutrients, phylogenetic diversity, functional evenness, freshwater mussel, consumer-driven nutrient dynamics, Unionidae, rivers/streams, stoichiometry

INTRODUCTION

Native biodiversity exerts many well-known positive influences on ecosystem functioning in both terrestrial (Tilman et al. 2001, Balvanera et al. 2006) and aquatic ecosystems (Duffy 2002, Cardinale 2011). Recent work, though, has indicated that functional diversity of organismal traits, as opposed to species richness, is a more robust determinant of ecological function (Petchey and Gaston 2006, Violle et al. 2007). Functional traits can be defined as any measurable phenotypic characteristic

(i.e., morphological, physiological) of an organism that influences ecological and evolutionary performances in nature (Violle et al. 2007, Diaz et al. 2013, Winemiller et al. 2015). Since traits affect ecosystem processes, a functional approach to studying biodiversity is fundamental to determine the mechanisms and evolutionary processes that have shaped current patterns of biodiversity (Loreau and de Mazancourt 2013, Winemiller et al. 2015).

Recent studies have also advocated that phylogenetic diversity, a measurement of distinct evolutionary history in a community, is a useful proxy for community-level functional diversity (Srivastava et al. 2012, Floeter et al. 2018). The relationship between phylogenetic and functional diversity is based on the hypothesis that trait diversification occurred due to evolutionary processes enhancing niche complementarity within communities (Srivastava et al. 2012). As a result, linking species traits and phylogeny has become commonplace in the ecological literature to make predictions regarding the evolutionary mechanisms linked to niche-partitioning and ecological function (Cadotte et al. 2009, Floeter et al. 2018). However, much of the work examining phylogenetic diversity, functional diversity, and ecological function has been focused on plant communities and little research to date has examined functional trait partitioning, diversity and divergence across animal phylogenies (but see, Floeter et al. 2018, González et al. 2018, Lamothe et al. 2018). Furthermore, these traits have rarely been explicitly linked to ecosystem functions that are relevant to other community members and ecological processes.

Ecological stoichiometry (ES) provides a framework to understand the balance of multiple key elements (commonly carbon [C], nitrogen [N], and phosphorus [P]) in ecological interactions and processes and can be used to infer relationships among the elemental composition of animals, their diet, and waste products (Sterner and Elser 2002, Atkinson et al. 2017). Animals preferentially sequester the element in shortest supply relative to demand and release relatively more of the element in excess (Boersma and Elser 2006, Frost et al. 2006) affecting the cycling and availability of nutrients in ecosystems (Atkinson and Vaughn 2015, Atkinson et al. 2017). A core concept of ES is strict homeostasis of consumer body tissues within the time scale at which ingestion, storage, and release of nutrients are being considered (Sterner and Elser 2002). In addition, the growth rate hypothesis states that during rapid growth, organisms contain more P-rich ribosomal RNA, thus faster-growing organisms are anticipated to have higher P concentrations in their tissue (Sterner and

Elser 2002). Consumer body tissue stoichiometry (i.e., the elemental ratio) is thus an important functional trait that has a predictable impact on nutrient cycling and availability (i.e., functional effect). A key knowledge gap is whether body tissue stoichiometry is coupled with phylogeny and may therefore mechanistically link evolutionary processes with ecosystem processes (see González et al. 2017, Peñuelas et al. 2019).

Species within the same feeding guild or phylogenetic grouping may differ dramatically in their traits and ecological functions, and ignoring these nuances may lead to poor evaluations of the ecosystem services and functions provided by organisms occupying similar functional guilds. Filter-feeding bivalves are a common functional feeding group in freshwater ecosystems and consist of a phylogenetically diverse assemblage of over 10 different bivalve families (Graf 2013). The most species-rich and ecologically important freshwater bivalve radiation in North America, the subfamily Ambleminae (~300 species in North America), are a group of long-lived (4 – 100 years), filter-feeding mollusks that occur in relatively distinct and dense multi-species aggregations (up to 200 individual m^{-2}) in freshwater ecosystems (Strayer 2008, Haag 2012). Mussel filter-feeding removes particulates and associated nutrients from the water column, concentrating materials in the benthic zone (Vaughn and Hoellein 2018) and their excretion is an important subsidy in nutrient-limited streams that facilitates algal growth (Atkinson et al. 2013, Atkinson et al. 2018), enhances secondary production (Vaughn and Spooner 2006), and results in biogeochemical hotspots through differential excretion of limiting and non-limiting nutrients (Atkinson and Vaughn 2015, Atkinson et al. 2017). The clear and global decline of freshwater mussel diversity and abundance (Lopes-Lima et al. 2018) has raised concerns about how ecological structure and function may be changing in aquatic ecosystems worldwide (Vaughn and Hoellein 2018).

Here we characterize niche variation and partitioning and the relationship between evolutionary history and ecological function by linking community composition, phylogeny, and species-level functional traits in a diverse, but highly imperiled faunal group. While freshwater mussels are generally assigned the same functional guild (i.e., filter-feeding bivalves), they vary tremendously in terms of their size, life span, growth rate, thermal tolerance, morphology, and other life history traits (Haag 2012, Spooner and Vaughn 2008). We used mussel soft tissue stoichiometry as our functional trait of interest by examining the stoichiometric niche of several species (as in

González et al. 2017) and determined ordinal stoichiometric distances (i.e., functional dissimilarity) among species pairs. Additionally, we calculated community-wide functional diversity metrics and determined if trait space corresponded to evolutionary history (i.e., phylogenetic dissimilarity). Body C:N:P is critical in understanding nutrient cycling because it can be used to determine the relative efficiencies with which two potentially limiting nutrients, N and P, will be recycled by animals (Sterner and Elser 2002, Atkinson et al. 2017). Thus, we also examined if tissue stoichiometry predicted an important functional effect trait, nutrient excretion stoichiometry. Given that mussel communities often occur in species-rich and dense aggregations (Strayer 2008, Haag 2012), we predicted that: 1) species would occupy distinct stoichiometric niches that vary as a result of evolutionary history; 2) stoichiometric variation among species would create distinct functional effects (i.e., nutrient excretion); and 3) communities with higher species and phylogenetic diversity would exhibit higher functional richness and greater trait dispersion.

METHODS

Field Sampling

We quantitatively sampled six sites with high freshwater mussel densities in the Sipsey River in July-October of 2016 (Sites 2-7) and one site in September 2018 (Site 1; Fig. 1A). The Sipsey River is a 2,044 km^2 alluvial river with extensive forested floodplain wetlands and is relatively unmodified by human activities and consequently has low background nutrient concentrations (Atkinson et al. 2019). The Sipsey River supports one of the most diverse and abundant freshwater communities left in the southeastern United States including most of its historical native mussel fauna (Haag and Warren 2010). We selected sites that were known to have mussels and first visually determined the extent of each mussel aggregation by snorkeling and then conducted quantitative sampling at each site within a 40-80 m stream reach depending on the size of the aggregation using a random start method. Each site was divided into 20-m sections (2-4 sections per site) in which three random numbers were selected within each 20-m section to determine our transects. Transects were run perpendicular to stream flow within each 20-m section (Appendix S1: Table S1). Across each transect (transect width range: 13.5-36.4 m) we excavated the sediment from a 0.25 m^2 quadrat to a depth of 15 cm every 1.5-m retaining all the material in a mesh bag. Each bag was individually labeled and all mussels were sorted through a series of sieves with individuals identified to species and their lengths recorded. Approximately

2.5% of the total area of the designated reach was sampled using this method. Mussel density, species richness, and the Shannon Diversity Index (H) were estimated from quadrat data for each community.

Water Chemistry, Tissue Stoichiometry, Excretion, and Egestion

We sampled ambient nutrient concentrations (ammonia and orthophosphate) at least twice at all sites between June and September 2016. Excretion rates for the nine most common species at our sites were measured in July–October 2016 and 2017 as a measurement of their functional effect on the ecosystem (N = 160). Excretion measurements were conducted in containers filled with 500 mL of filtered river water (GF/F; 0.7 um pore size; EMD Millipore, Buckinghamshire, U.K.) following Atkinson et al. (2013). Mussels were gently scrubbed under water to remove biofilm, and one individual mussel was used in each excretion chamber. Empty, scrubbed mussel shells collected from the stream were used as a control for the presence of an object in the chambers and the potential of associated algae and bacteria passing through the filter. Scrubbed mussels and shells were removed from containers after an hour, and the water from each container was filtered through a GF/F filter (0.7 μm pore size; Millipore) to separate egestion products (i.e. biodeposits), collected on the filter, from soluble nutrients (i.e. the filtrate-excreta). We dried egesta filters to a constant weight at 50 °C, weighed them on an analytical balance, and analyzed for %C,%N, and %P as described below for mussel tissue. Water samples for excretion were analyzed for ammonia and orthophosphate using a Lachat QuikChem FIA +8000 Series flow injection analyzer (Hach Company, Loveland, CO, U.S.A.). Excretion rates were calculated based on the difference in dissolved nutrient concentrations between the control and mussel containers following a 1-h incubation. Mass-specific excretion and egestion rates were calculated by dividing the observed excretion rate by the soft-tissue dry mass (in grams) of each individual and ratios are reported as molar ratios.

Following the excretion measurements, a subset of mussels of ten species (i.e., *Truncilla donaciformes* was only collected at one site for tissue chemistry only) were placed on ice and returned to the laboratory (n = 183). Length, total wet mass, and soft tissue dry mass were determined for each individual. We determined tissue nutrient composition (%C, %N, and %P) as a functional trait of each species. We measured C:N using dry, homogenized samples on a Carlo Erba CHNS-O EA1108-Elemental Analyzer (Isomass Scientific Inc., Calgary, Alberta, Canada). For %P, dry samples were weighed, combusted at 500 °C for 2 h, and analyzed with HCl digestion followed by soluble reactive

P analysis. The C, N, and P composition was then converted to molar ratios to express stoichiometric ratios. Body nutrient composition was measured for 183 individuals of ten species and the nutrient composition of egestion and excretion were measured for 160 of nine species of those same individuals.

Phylogenetic Analyses

We assembled a molecular phylogenetic matrix consisting of each unionid species in the Sipsey River by downloading previous published cytochrome oxidase subunit I (COI) gene fragments from Genbank (Appendix S1: Table S2). There were no publicly available molecular data for *Lasmigona alabamensis* and *Cyclonaias asperata*, so we utilized closely related species as proxies (*Lasmigona complanata* and *Cyclonaias pustulosa*, respectively). Sequences were aligned in Mesquite v 3.10 (Maddison and Maddison 2016) using MUSCLE (Edgar 2004). PartitionFinder v2.1.1 (Lanfear et al. 2016) was used to find the best partitioning scheme of the possible subsets (one per codon position) and the best gamma model of nucleotide substitution using the AICc selection criterion and the greedy search algorithm. Maximum likelihood (ML) analyses were implemented in RAXML v 8.2.8 (Stamatakis 2014) using the best partitioning scheme and model of nucleotide evolution and 1000 tree searches. We calculated a phylogenetic distance matrix using the best ML tree and the cophenetic function in the R package ape v 5.1 (Paradis et al. 2004). The resulting phylogenetic distance matrix was then parsed down to only include species in which we had corresponding tissue stoichiometry (Table 1).

Stoichiometric Niche as a Functional Trait across Species

We used the %C, %N, and %P composition as metrics of functional trait diversity in our system. These are meaningful measures as the tissue stoichiometry of unionid mussels can strongly affect nutrient excretion stoichiometry (Atkinson et al. 2014, Atkinson and Vaughn 2015). We used a mixed-effects model implemented in 'lme4' with site as a random effect to determine if body tissue %C, %N, %P, C:N, C:P, and N:P varied across the ten taxa. We used Satterthwaite's method to estimate *P*-values and degrees of freedom. Significant differences were followed by Tukey's post-hoc tests as implemented in the 'multcomp' function. We visualized the stoichiometric composition of nine study species (*Truncilla donaciformes* excluded) in multivariate space to quantify stoichiometric niche dimensions (González et al. 2017). We calculated stoichiometric niche volumes occupied by

each of our species to estimate stoichiometric diversity within our mussel communities as represented by their %C, %N and %P values in three-dimensional space. We then evaluated the complementarity in mussel stoichiometric niches by measuring the percent overlap among species' stoichiometric niches (González et al. 2017). Specifically, the niche overlap between two species was calculated as the ratio of the niche volume in common to the combined unique niche volume (i.e., sum of the two niche volumes minus the volume of the intersection). Nestedness of two niche volumes was calculated as the ratio between the overlapped niche volume and the minimal niche volume occupied by a group (Villéger et al. 2011). Nestedness values ranged between 0 and 1; a value of 0 suggests that niche volumes do not overlap and a value of 1 is when a given niche volume is nested and occupies a small portion of a larger niche volume displayed by a second group (Villéger et al. 2011). Stoichiometric niche analyses were performed using the packages geometry, car, coin, rcdd, and the function CHVintersect in R v3.3.1 (R Core Team 2018).

Functional Diversity and Dissimilarity across Species

To characterize the functional stoichiometric trait divergence, as represented by C:N, C:P, and N:P molar ratios, we used a distance-based measure across our ten species pool. We natural log-transformed body stoichiometry trait data and then scaled the data using a principal components analysis to eliminate trait redundancy as advised by Swenson (2014). The resulting first two PC axes of function were used to calculate a multivariate Euclidean distance between all species measured. To explore if tissue stoichiometry varied as a function of phylogenetic distance, we used linear regression to determine if phylogenetic distance between each of our species pairs predicted functional dissimilarity as estimated by stoichiometric trait divergence. We followed this with Bloomberg's K and Pagel's λ to estimate the phylogenetic signal for each stoichiometric trait (Table 1) using the 'phytools' function 'phylosig' (Revell, 2012). The stochiometric dissimilarity matrix was used to create a dendrogram using 'hclust' which was visualized together with our molecular topology using the 'phytools' function 'cophylo'. As the growth rate hypothesis predicts that faster growing organisms will have higher %P, we used linear regression to examine if average growth rate (K) across these species was a driver of body %P. While growth rates can be plastic in response to environmental gradients (e.g., Boersma et al. 2006), we used average growth rates (K) that were obtained for each species in which the data were specific for mussel species from our study system,

the Sipsey River (Haag and Rypel 2011). Following this, we determined if tissue N:P predicted functional effect traits, excretion N:P and egestion N:P, using linear regression on data from individuals with paired measurements (N = 160). We also examined if tissue C:N and C:P predicted egestion C:N or C:P using linear regression.

Phylogenetic and Functional Diversity across Communities

We calculated Faith's phylogenetic diversity of each site using the 'pd' function in the R package 'picante' (Kembel et al. 2010). We then examined the phylogenetic structure across our communities by calculating the mean pairwise phylogenetic distance (MPD) and mean nearest taxon phylogenetic distance (MNTD) among species in each study site. These indices were compared to null models to test whether the phylogenetic and structure differed from random expectations by calculating standardized effect sizes (SES_{MPD} and SES_{MNTD}; Kembel et al. 2010). We also examined functional diversity across the seven mussel communities using the metrics of functional evenness (F_{Eve}) and functional dispersion (F_{Dis}). Functional evenness measures the regularity of species traits along the trait distance matrix space and the regularity of their biomass across communities. Functional dispersion is a metric of functional structure and calculates the distance of each community species combination from the centroid of the community traits. F_{Eve} and F_{Dis} were calculated using the dbFD() function in the R package FD. To determine if phylogenetic diversity or species diversity was related to functional diversity, we examined relationships between typical diversity metrics (i.e., species richness and Shannon diversity), phylogenetic diversity, and functional diversity metrics (F_{Eve}, and F_{Dis}) of the communities using linear and non-linear regression. We calculated the biomass-weighted mean and standard deviation for each stoichiometric functional traits (C:N, C:P, N:P) for each community and used a one-way ANOVA to determine if it varied across the seven communities.

RESULTS

Species Diversity

Across seven sites, we excavated 1,031 0.25m^2 quadrats and identified and measured 7,273 individual live mussels representing 30 species (Fig. 1A). Species richness across sites varied from 15 (Site 1) to 29 (Site 7) species and average site density site ranged 11-38 individuals m^{-2} (Fig. 1B; Appendix S1: Table S1). Across all sites, *Pleurobema decisum*, *Cyclonaias asperata*, and *Fusconaia cerina*

dominated numerically and our ten taxa comprised 78%-89% of the total mussel community abundance (Fig. 1C). Shannon diversity was lowest at Site 5 (H = 1.67), while the highest value was from Site 7 (H = 2.07), the most downstream site (Appendix S1: Table S1).

Tissue Stoichiometry and Niche Space

Mussel tissue %C (Fig. 2A; $F_{9,170}$ = 6.0, $P < 0.0001$) , %N (Fig. 2B; $F_{9, 170}$ = 3.4, $P < 0.001$), and %P (Fig. 2C; $F_{9, 172}$ = 7.1, $P < 0.0001$) varied across species. As a result of the variation in elemental composition across species, there were also differences C:N (Fig. 2D; $F_{9, 170}$ = 9.7, $P < 0.0001$), C:P (Fig. 2E; $F_{9, 170}$ = 9.2, $P < 0.0001$), and N:P (Fig. 2F; $F_{9,170}$ = 6.7, $P < 0.0001$). In general, Lampsilini species tended to have lower C:N and C:P values (except *Obliquaria reflexa*) and Quadrulini species had higher C:N and C:P values. Three species in the Lampsilini tribe, *Lampsilis ornata*, *Obovaria unicolor* and *Obliquaria reflexa,* occupied the greatest stoichiometric niche space as represented by their total convex hull volume (37.4, 27.2, and 8.7, respectively; Fig. 3A; Appendix S1: Table S3). This pattern was followed by two common Quadrulini species, *Tritogonia verrucosa* and *Cyclonaias asperata* (convex hull volume = 7.6 and 6.7, respectively), occupying 5.8% and 5.1% of the total niche hull volume, respectively. The three Pleurobemini species, including the most dominant species, *Pleurobema decisum* (convex hull volume = 4.5), occupied a total of 10.2% of the stoichiometric niche volume. *Amblema plicata* (Amblemini Tribe) had a small convex hull volume (0.3) and occupied the rest of the total niche volume (0.6%). We observed partitioning in stoichiometric niches across species with overlap across each species pair being an average of 11.8 ± 8.7% (mean ± standard error). *Tritogonia verrucosa* had the highest degree of overlap, sharing 25% of stoichiometric niche space with another Quadrulini species, *Cyclonaias asperata*. Nestedness ranged from <0.01 to 0.79 (average= 0.28) with higher nestedness within species pairs that occupied the same phylogenetic tribe (Appendix S1: Table S3).

Phylogenetic Patterns in Functional Traits and Functional Effect Traits

The most likely species topology recovered in our ML analysis (Appendix S1: Fig. S1) was acquired by partitioning by codon position and using the GTR+G model for each partition. The resultant topology is similar to recent phylogenetic reconstructions of the subfamily Ambleminae (Pfeiffer et al. 2019a, Pfeiffer et al. 2019b) and represents a useful estimation to measure phylogenetic diversity and dissimilarity in the assemblage. There was a significant positive relationship between

phylogenetic dissimilarity and functional trait dissimilarity across species pairs (Fig. 3B; $y = 0.99x + 0.99r^2 = 0.13$; $P = 0.02$). We found varying levels of phylogenetic signal associated with the measured stochiometric ratios, with N:P having a moderate to strong phylogenetic signal, and C:N and C:P having little to moderate phylogenetic signal as indicated by Bloomberg's K and Pagel's λ (Appendix S1: Table S4). Growth rate, a hypothesized driver of tissue stoichiometry, was a positive predictor of body %P content (Fig. 3C; $y = 2.34x + 1.61$; $r^2 = 0.64$; $P = 0.009$). The tissue N:P was a strong driver of excretion N:P (Fig. 3D; $y = 94.13\text{-}5.69x$; $r^2 = 0.60$; $P = 0.01$), with low tissue N:P (mostly Lampsilini) producing higher excretion N:P and high tissue N:P (mostly Pleurobemini and *Amblema plicata*) producing lower excretion N:P. Excretion N:P of all species exceeded background N:P in the water column (Appendix S1: Table S1). Egestion C:N, C:P, and N:P (Table 1) were not predicted by tissue stoichiometry ($P > 0.5$ in all cases). Functional dissimilarity represented by tissue stoichiometry did correlate in most instances with the phylogeny, further suggesting a phylogenetic signal in mussel tissue stoichiometry (Fig. 4).

Community Phylogenetic Diversity and Functional Trait Evenness and Dispersion

Expectedly, phylogenetic diversity at each site was similar to species richness with Sites 1 and 7 having the lowest and highest diversity, respectively (Fig 5A; $r^2 = 0.97$; $P < 0.0001$; Appendix S1: Table S1). Sites 4 and 7 both had the highest functional trait evenness (both F_{Eve} ~0.76), and Site 1 had the lowest ($F_{Eve} = 0.44$). One of the upstream sites, Site 2, had the greatest community-level functional trait dispersion, while the most downstream site, Site 7, had the lowest dispersion (Appendix S1: Table S1). F_{Dis} was greatest at intermediate species richness (Fig 5B; $r^2 = 0.98$; $P < 0.001$) and strongly negatively correlated to Shannon Diversity (Fig 5C; $r^2 = 0.92$; $P < 0.001$). F_{Dis} was also greatest at intermediate phylogenetic diversity (Fig 5D; $r^2 = 0.98$; $P < 0.001$). F_{Eve} was not significantly related to species richness ($P = 0.17$), Shannon Diversity ($P = 0.10$), or phylogenetic diversity ($P = 0.13$). The communities sampled here were generally phylogenetically clustered as SES_{MPD} and SES_{MNTD} values were negative in comparison to a null model (Appendix S1: Table S1). Overall, community composition was similar across our sites as indicated by our diversity metrics and so was overall function, thus the resulting community-weighted tissue C:N, C:P, and N:P did not vary across sites (ANOVA, $P > 0.05$; Appendix S1: Fig. S2).

DISCUSSION

Species stoichiometry in animals tends to be a taxon-dependent homeostatic trait that ultimately arises from evolutionary pressures on form and ecological function (Sterner and Elser 2002, Jeyasingh et al. 2014, Peñuelas et al. 2019). Our results show considerable differences and phylogenetic signal in important functional traits and consequential functional effect traits within co-occurring species (Fig. 3A, Fig. 3D) that are commonly classified within the same guild or functional feeding group (i.e., filter-feeding bivalves). Previous work has shown that stoichiometric variation results from taxonomic identity (González et al. 2018), but this pattern has typically been studied at higher organizational levels above the family-level (Vanni and McIntyre 2016). Our results show that even within a relatively shallow clade of filter-feeding freshwater bivalves, co-occurring species occupy distinct stochiometric niches (Fig. 3A) having a direct impact on nutrient remineralization stoichiometry (Fig 3D). We demonstrate that tissue stoichiometry, an important functional trait, is partially attributable to evolutionary history and is conserved within a single subfamily (Fig. 4), as more phylogenetically divergent species had greater divergence in their tissue stoichiometric signature (Fig. 3B). Our findings highlight that adaptive radiation within a subfamily has led to distinct stoichiometric niches and functional effects that have ecosystem-level consequences (Atkinson et al. 2014, Atkinson et al. 2018).

One of the major evolutionary factors that has been hypothesized to influence the stoichiometry of animals is the growth rate hypothesis, which suggests that there are positive correlations among P content and growth rate. The growth rate hypothesis appears to be an important factor operating as %P of mussel soft tissue was positively correlated to previously documented average growth rates (Fig. 3C). For example, our faster growing species of the Lampsilini (see Haag and Rypel 2011), had higher body %P, and as a result lower tissue C:P and N:P (Fig 3D). This lower tissue N:P resulted in higher excretion N:P. We suggest that since tissue stoichiometry, especially N:P, varies as a result of life history characteristics, it is a powerful tool for examining the congruence between evolutionary history and trait variation, and their consequential effects of community assembly and ecosystem function. Recent work in ES and consumer-driven nutrient dynamics has shown a large degree of intra- and interspecific variation in tissue and nutrient recycling stoichiometry (El-Sabaawi et al. 2015, Balik et al. 2018, Dalton et al. 2018) and further research across taxa,

populations, and life stages will help elucidate the patterns and processes associated with stoichiometric niche partitioning.

Not surprisingly, we found a positive relationship between species richness and phylogenetic diversity (Fig 5A) as found in other studies (Cadotte and Tucker 2017). However, contrary to our predictions, we found that community species richness and phylogenetic diversity displayed a unimodal relationship with functional dispersion of stoichiometric traits as opposed to a positive relationship. While generally there was a positive relationship, there was a threshold in which functional dispersion peaked, but then declined with species richness (Fig 5B) and phylogenetic diversity (Fig 5D). Previous work has found that functional dispersion increases with species richness (Tsianou and Kallimanis 2020) often increasing to a threshold (Laliberté and Legendre 2010, Lamothe et al. 2018). Our results may be partially attributable to working within a single river system with our communities being relatively similar as a result of a restricted regional species pool. Examining patterns in functional dispersion across scales will be essential for determining the mechanisms generating patterns in community assembly and function.

We clearly showed interspecific differences in tissue stoichiometry with high variation in the total stoichiometric niche space occupied by each species (Fig. 3A). Mussel communities here varied in overall species richness and density, but generally were dominated by long-lived species with late maturity (i.e., equilibrium strategy sensu Haag 2012; Table 1, Fig 1A). Equilibrium species tended to have small stoichiometric niche volumes with limited niche overlap, a pattern consistent with substantial niche partitioning shaped by directional selection acting to reduce niche overlap (Sterner and Elser 2002, González et al. 2017). This was contrasted by species with a periodic life history strategy that tended to have greater stoichiometric overlap and larger niche volumes, including several representatives of the Lampsilini (e.g., *Lampsilis ornata, Obovaria unicolor, Obliquaria reflexa,* Fig. 3A). Lampsilines often have fast growth rates, shorter life spans, early sexual maturation, and high variability in annual recruitment, traits that are hypothesized to facilitate persistence in more variable and less stable habitats (periodic strategy; Table 1, Fig 1A; Haag 2012). Given the life history characteristics of these species, it is logical to hypothesize that they may be better adapted to use a broad food resource base. More work contrasting life history variation across taxa is critical in

understanding the mechanisms determining intra- and interspecific variation in tissue stoichiometry and their consequential impacts on nutrient cycling and other ecosystem functions.

In addition to functional traits and functional effect traits, organisms vary greatly in their response traits, or the ability of an organism to persist due to environmental challenges (Chessman 2013, Diaz et al. 2013). For example, freshwater mussel species vary in their response to thermal stress (i.e., some being sensitive or tolerant to drought and heat; Spooner and Vaughn 2008), which can result in dramatic community shifts (Atkinson et al. 2014). The focal communities studied here are dominated by slow-growing, long-lived, late-maturing species (Fig 1C; Haag and Rypel 2011) that are favored in low disturbance environments (Haag 2012). Most climate change projections for the southeastern US predict increasing drought and that the frequency of both above- and below-median flows will increase (Golladay et al. 2016), suggesting an increase in disturbance frequency. Given these projections, we may anticipate shifts in communities dominated by long-lived, equilibrium species to communities dominated by short-lived periodic species based on life-history strategies (DuBose et al. 2019). However, predictions based on response traits may be in conflict to those made based on life history strategies. For example, in the aforementioned scenario we might expect an increase in abundance of short-lived lampsilines. However, previous research indicates that lampsilines may be among the most thermally sensitive groups of unionid mussels (Spooner and Vaughn 2008). Thus, teasing apart the relative importance of life history versus response traits will be critical for discerning the functional traits and functional effect traits that will be maintained in freshwater ecosystems. Given the high diversity of species within this single functional guild, our work suggests that species rich and phylogenetically diverse communities may act to stabilize ecosystem functioning in the face of global change (similar to Tilman et al. 2006, Loreau and de Mazancourt 2013).

While our study was confined to a single river, our results indicate that significant stoichiometric niche variation occurs in these closely related filter-feeding bivalves. More work needs to be conducted to elucidate if the stoichiometric niche patterns and resultant functional effects of nutrient regeneration found here translates across different river systems and species, or if there are distinct intraspecific effects driven by the environment. Along this same line of thought, do phylogenetically related species across systems have more similar stoichiometric traits? These

patterns in organismal nutrient assimilation and regeneration need to be examined more broadly to determine the mechanisms underlying stoichiometric niche partitioning and the role it plays in biogeochemical cycling across broad spatial scales. Further examination of these patterns will help ecologists and evolutionary biologists understand the relative role of evolutionary history, plasticity, and environmental variation in determining how species and phylogenetic diversity contributes to ecological function.

ACKNOWLEDGEMENTS

This work would not have been possible without field assistance from Mark Dedmon, Anne Marie Green, Clay Magnum, Jami Nettles, Zach Nickerson, Lauren Shouse, Nate Sturm, and Chloe Atkinson. Anne Bell assisted with the water chemistry analyses. Kelly Lambert provided freshwater mussel illustrations. We appreciate comments on previous versions of this manuscript from Halvor Halvorson, Garrett Hopper, Jeff Lozier, Caryn Vaughn, Olivier Dézerald, Helmut Hillebrand, and two anonymous reviewers. The Weyerhaeuser Company, Alabama Department of Natural Resources and Conservation, and National Science Foundation DEB-1831512 provided support for this project. Freshwater mussel collection was conducted under USFWS permit #TE68616B-1 and ALCDNR permit #2016077745468680.

LITERATURE CITED

Atkinson, C. L., K. A. Capps, A. T. Rugenski, and M. J. Vanni. 2017. Consumer-driven nutrient dynamics in freshwater ecosystems: from individuals to ecosystems. Biological Reviews **92**:2003-2023.

Atkinson, C. L., J. P. Julian, and C. C. Vaughn. 2014. Species and function lost: Role of drought in structuring stream communities. Biological Conservation **176**:30-38.

Atkinson, C. L., B. J. Sansom, C. C. Vaughn, and K. J. Forshay. 2018. Consumer aggregations drive nutrient dynamics and ecosystem metabolism in nutrient-limited systems. Ecosystems **21**:521-535.

Atkinson, C. L., B. C. van Ee, Y. Lu, and W. Zhong. 2019. Wetland floodplain flux: temporal and spatial availability of organic matter and dissolved nutrients in an unmodified river. Biogeochemistry **142**:395-411.

Atkinson, C. L., and C. C. Vaughn. 2015. Biogeochemical hotspots: temporal and spatial scaling of the impact of freshwater mussels on ecosystem function. Freshwater Biology **60**:563-574.

Atkinson, C. L., C. C. Vaughn, K. J. Forshay, and J. T. Cooper. 2013. Aggregated filter-feeding consumers alter nutrient limitation: Consequences for ecosystem and community dynamics. Ecology **94**:1359-1369.

Balik, J. A., B. W. Taylor, S. E. Washko, and S. A. Wissinger. 2018. High interspecific variation in nutrient excretion within a guild of closely related caddisfly species. Ecosphere **9**:e02205.

Balvanera, P., A. B. Pfisterer, N. Buchmann, J. S. He, T. Nakashizuka, D. Raffaelli, and B. Schmid. 2006. Quantifying the evidence for biodiversity effects on ecosystem functioning and services. Ecology Letters **9**:1146-1156.

Boersma, M., and J. J. Elser. 2006. Too much of a good thing: On stoichiometrically balanced diets and maximal growth. Ecology **87**:1325-1330.

Cadotte, M. W., J. Cavender-Bares, D. Tilman, and T. H. Oakley. 2009. Using phylogenetic, functional and trait diversity to understand patterns of plant community productivity. PloS one **4**:e5695.

Cadotte, M. W., and C. M. Tucker. 2018. Difficult decisions: Strategies for conservation prioritization when taxonomic, phylogenetic and functional diversity are not spatially congruent. Biological Conservation **225**:128-133.

Cardinale, B. J. 2011. Biodiversity improves water quality through niche partitioning. Nature **472**:86-U113.

Chessman, B. C. 2013. Identifying species at risk from climate change: Traits predict the drought vulnerability of freshwater fishes. Biological Conservation **160**:40-49.

Dalton, C. M., K. E. Tracy, N. G. Hairston Jr, and A. S. Flecker. 2018. Fasting or fear: Disentangling the roles of predation risk and food deprivation in the nitrogen metabolism of consumers. Ecology **65**:394-400.

Diaz, S., A. Purvis, J. H. C. Cornelissen, G. M. Mace, M. J. Donoghue, R. M. Ewers, P. Jordano, and W. D. Pearse. 2013. Functional traits, the phylogeny of function, and ecosystem service vulnerability. Ecology and Evolution **3**:2958-2975.

DuBose, T. P., C. L. Atkinson, C. C. Vaughn, S. W. Golladay. 2019. Drought-induced, punctuated loss of freshwater mussels alters ecosystem function across temporal scales. Frontiers in Ecology and Evolution 7:274.

Duffy, J. E. 2002. Biodiversity and ecosystem function: the consumer connection. Oikos **99**:201-219.

Edgar, R. C. 2004. MUSCLE: multiple sequence alignment with high accuracy and high throughput. Nucleic Acids Research **32**:1792-1797.

El-Sabaawi, R. W., M. C. Marshall, R. D. Bassar, A. López-Sepulcre, E. P. Palkovacs, and C. Dalton. 2015. Assessing the effects of guppy life history evolution on nutrient recycling: from experiments to the field. Freshwater Biology **60**:590-601.

Floeter, S. R., M. G. Bender, A. C. Siqueira, and P. F. Cowman. 2018. Phylogenetic perspectives on reef fish functional traits. Biological Reviews **93**:131-151.

Frost, P. C., J. P. Benstead, W. F. Cross, H. Hillebrand, J. H. Larson, M. A. Xenopoulos, and T. Yoshida. 2006. Threshold elemental ratios of carbon and phosphorus in aquatic consumers. Ecology Letters **9**:774-779.

Golladay, S., K. Martin, J. Vose, D. Wear, A. Covich, R. Hobbs, K. Klepzig, G. Likens, R. Naiman, and A. Shearer. 2016. Achievable future conditions as a framework for guiding forest conservation and management. Forest Ecology and Management **360**:80-96.

González, A. L., R. Céréghino, O. Dézerald, V. F. Farjalla, C. Leroy, B. A. Richardson, M. J. Richardson, G. Q. Romero, and D. S. Srivastava. 2018. Ecological mechanisms and phylogeny shape invertebrate stoichiometry: A test using detritus-based communities across Central and South America. Functional Ecology **32**:2448-2463.

González, A. L., O. Dézerald, P. A. Marquet, G. Q. Romero, and D. S. Srivastava. 2017. The multidimensional stoichiometric niche. Frontiers in Ecology and Evolution **5**:110.

Graf, D. L. 2013. Patterns of freshwater bivalve global diversity and the state of phylogenetic studies on the Unionoida, Sphaeriidae, and Cyrenidae. American Malacological Bulletin **31**:135-153, 119.

Haag, W. R. 2012. North American Freshwater Mussels: Ecology, Natural History, and Conservation. Cambridge University Press, New York, NY.

Haag, W. R., and A. L. Rypel. 2011. Growth and longevity in freshwater mussels: evolutionary and conservation implications. Biological Reviews **86**:225-247.

Haag, W. R., and M. L. Warren. 2010. Diversity, abundance, and size structure of bivalve assemblages in the Sipsey River, Alabama. Aquatic Conservation: Marine and Freshwater Ecosystems **20**:655-667.

Jeyasingh, P. D., R. D. Cothran, and M. Tobler. 2014. Testing the ecological consequences of evolutionary change using elements. Ecology and Evolution **4**:528-538.

Kembel, S. W., P. D. Cowan, M. R. Helmus, W. K. Cornwell, H. Morlon, D. D. Ackerly, S. P. Blomberg, and C. O. Webb. 2010. Picante: R tools for integrating phylogenies and ecology. Bioinformatics **26**:1463-1464.

Laliberté, E., and P. Legendre. 2010. A distance-based framework for measuring functional diversity from multiple traits. Ecology **91**:299-305.

Lamothe, K. A., K. M. Alofs, D. A. Jackson, and K. M. Somers. 2018. Functional diversity and redundancy of freshwater fish communities across biogeographic and environmental gradients. Diversity and Distributions **24**:1612-1626.

Lanfear, R., P. B. Frandsen, A. M. Wright, T. Senfeld, and B. Calcott. 2016. PartitionFinder 2: new methods for selecting partitioned models of evolution for molecular and morphological phylogenetic analyses. Molecular Biology and Evolution **34**:772-773.

Lopes-Lima, M., L. E. Burlakova, A. Y. Karatayev, K. Mehler, M. Seddon, and R. Sousa. 2018. Conservation of freshwater bivalves at the global scale: diversity, threats and research needs. Hydrobiologia **810**:1-14.

Loreau, M., and C. de Mazancourt. 2013. Biodiversity and ecosystem stability: a synthesis of underlying mechanisms. Ecology Letters **16**:106-115.

Maddison, W. P., and D. R. Maddison. 2016. Mesquite: a modular system for evolutionary analysis. Version 3.10

Paradis, E., J. Claude, and K. Strimmer. 2004. APE: analyses of phylogenetics and evolution in R language. Bioinformatics **20**:289-290.

Peñuelas, J., M. Fernández-Martínez, P. Ciais, D. Jou, S. Piao, M. Obersteiner, S. Vicca, I. A. Janssens, and J. Sardans. 2019. The bioelements, the elementome, and the biogeochemical niche. Ecology:e02652.

Petchey, O. L., and K. J. Gaston. 2006. Functional diversity: back to basics and looking forward. Ecology letters **9**:741-758.

Pfeiffer, J. M., C. L. Atkinson, A. E. Sharpe, K. A. Capps, K. F. Emery, and L. M. Page. 2019a. Phylogeny of Mesoamerican freshwater mussels and a revised tribe-level classification of the Ambleminae. Zoologica Scripta **48**:106-117.

Pfeiffer, J. M., J. W. Breinholt, and L. M. Page. 2019b. Unioverse: A phylogenomic resource for reconstructing the evolution of freshwater mussels (Bivalvia, Unionoida). Molecular Phylogenetics and Evolution.

R Core Team. 2018. R: A language and environment for statistical computing. R Foundation for Statistical Computing, Vienna, Austria.

Revell, L. J. 2012. phytools: An R package for phylogenetic comparative biology (and other things). Methods in Ecology and Evolution **3**:217-223.

Spooner, D. E., and C. C. Vaughn. 2008. A trait-based approach to species' roles in stream ecosystems: climate change, community structure, and material cycling. Oecologia **158**:307-317.

Srivastava, D. S., M. W. Cadotte, A. A. M. MacDonald, R. G. Marushia, and N. Mirotchnick. 2012. Phylogenetic diversity and the functioning of ecosystems. Ecology Letters **15**:637-648.

Stamatakis, A. 2014. RAxML version 8: a tool for phylogenetic analysis and post-analysis of large phylogenies. Bioinformatics **30**:1312-1313.

Sterner, R. W., and J. J. Elser. 2002. Ecological Stoichiometry: The Biology of Elements from Molecules to the Biosphere. Princeton University Press, Princeton, NJ.

Strayer, D. L. 2008. Freshwater Mussel Ecology: A Multifactor Approach to Distribution and Abundance. University of California Press, Berkeley, CA.

Swenson, N. G. 2014. Functional and phylogenetic ecology in R. Springer, New York, NY.

Tilman, D., P. B. Reich, J. Knops, D. Wedin, T. Mielke, and C. Lehman. 2001. Diversity and productivity in a long-term grassland experiment. Science **294**:843-845.

Tilman, D., P. B. Reich, and J. M. Knops. 2006. Biodiversity and ecosystem stability in a decade-long grassland experiment. Nature **441**:629.

Tsianou, M. A., and A. S. Kallimanis. 2020. Geographical patterns and environmental drivers of functional diversity and trait space of amphibians of Europe. Ecological Research **35**:123-138.

Vanni, M. J., and P. B. McIntyre. 2016. Predicting nutrient excretion of aquatic animals with metabolic ecology and ecological stoichiometry: a global synthesis. Ecology **97**:3460-3471.

Vaughn, C. C., and T. J. Hoellein. 2018. Bivalve Impacts in Freshwater and Marine Ecosystems. Annual Review of Ecology, Evolution, and Systematics **49**:183-208.

Vaughn, C. C., and D. E. Spooner. 2006. Unionid mussels influence macroinvertebrate assemblage structure in streams. Journal of the North American Benthological Society **25**:691-700.

Villéger, S., P. M. Novack-Gottshall, and D. Mouillot. 2011. The multidimensionality of the niche reveals functional diversity changes in benthic marine biotas across geological time. Ecology Letters **14**:561-568.

Violle, C., M. L. Navas, D. Vile, E. Kazakou, C. Fortunel, I. Hummel, and E. Garnier. 2007. Let the concept of trait be functional! Oikos **116**:882-892.

Winemiller, K. O., D. B. Fitzgerald, L. M. Bower, and E. R. Pianka. 2015. Functional traits, convergent evolution, and periodic tables of niches. Ecology Letters **18**:737-751.

Table 1. Phylogenetic tribe grouping (see Appendix 1: Fig. S1 for phylogenetic tree), life history strategy (Haag 2012), the number of individuals per species in which we measured body tissue nutrient composition (mean ± standard error) of ten common freshwater mussel species occupying the Sipsey River, Alabama, USA. We also report the mean excretion and biodeposit stoichiometric ratios (± standard error) for the individuals in which excretion and biodeposit measurements were made (N = 160). Excretion and egestion were not measured for *Truncilla donaciformes*.

Species	Phylogenetic Tribe	Life History Strategy	N	Tissue C:N	Tissue C:P	Tissue N:P	Excretion N:P	Biodeposit C:N	Biodeposit C:P	Biodeposit N:P
Amblema plicata	Amblemini	Equilibrium	10	5.52 ± 0.13	62.30 ± 3.26	11.40 ± 0.83	22.28 ± 7.00	35.73 ± 10.10	327.59 ± 253.68	100.88 ± 31.90
Cyclonaias asperata	Quadrulini	Equilibrium	30	5.66 ± 0.06	59.10 ± 2.34	10.50 ± 0.40	33.88 ± 3.49	24.62 ± 7.29	79.73 ± 194.65	21.02 ± 3.55
Elliptio arca	Pleurobemini	Periodic	10	5.21 ± 0.03	53.59 ± 2.86	10.25 ± 0.75	39.95 ± 4.21	5.94 ± 0.19	177.24 ± 56.05	30.26 ± 9.57
Fusconaia cerina	Pleurobemini	Equilibrium	29	5.32 ± 0.05	59.93 ± 2.71	11.32 ± 0.43	35.12 ± 3.51	5.78 ± 0.20	561.88 ± 189.85	236.07 ± 43.10
Lampsilis ornata	Lampsilini	Periodic	30	4.73 ± 0.05	39.59 ± 0.99	8.35 ± 0.45	44.97 ± 5.21	5.84 ± 0.18	333.97 ± 60.97	63.99 ± 11.68
Obliquaria reflexa	Lampsilini	Periodic	15	5.97 ± 0.07	51.23 ± 2.09	8.62 ± 0.50	50.78 ± 1.34	5.74 ± 0.43	47.68 ± 10.66	8.06 ± 1.80
Obovaria unicolor	Lampsilini	Periodic	25	5.38 ± 0.14	45.83 ± 0.31	8.54 ± 0.29	46.64 ± 1.22	66.93 ± 5.52	168.93 ± 33.79	2.39 ± 0.48

Pleurobema decisum	Pleurobemini	Equilibrium	15	5.03 ± 0.07	48.58 ± 2.84	9.66 ± 0.70	28.18 ± 4.86	16.61 ± 11.69	178.27 ± 291.59	258.34 ± 66.70
Tritogonia verrucosa	Quadrulini	Periodic	15	5.42 ± 0.14	56.45 ± 2.95	10.43 ± 0.47	34.23 ± 3.42	7.69 ± 0.18	230.47 ± 51.53	29.38 ± 6.56
Truncilla donaciformes	Lampsilini	Opportunistic	4	5.24 ± 0.19	42.18 ± 2.99	8.05 ± 0.88	NA	NA	NA	NA

Fig. 1. Species composition of study sites. (A) Sites used in the study with the species proportional abundance at each site. Species that have an equilibrium life history strategy (Haag 2012) are indicated with an asterisk. (B) Freshwater mussel species richness and (C) densities of the ten most common species at each of our sites.

Fig. 2. Boxplots of the soft tissue chemistry of the ten study species including (A) %C, (B) %N, (C) %P, (D) molar C:N, (E) molar C:P and (F) molar N:P. Species are color coded by their phylogenetic tribe: Amblemini (blue), Lampsilini (green), Pleurobemini (orange) and Quadrulini (black). Letters to the right of the boxplots indicate results from Tukey's post *hoc* tests following significant mixed effect models. The line within the box represents the median and the maximim and minimum line making up the box represents the third and first quantile, respectively. The lines extending outside of the box extend to the minimum and maximum values.

Fig. 3. (A) The stoichiometric niches of the nine species used in the stoichiometric niche analysis. Sphere size indicates the relative stoichiometric niche volume and are centered around the average C, N and P contents of each species. Species are ordered by their stoichiometric niche size, with *Lampsilis ornata*, a Lampsilini having the largest hull volume and *Amblema plicata*, the only Amblemini, having the smallest hull volume. Dots indicate individual coordinates and show the variability in each species' stoichiometric niche. (B) The relationship between phylogenetic dissimilarity and functional dissimilarity (i.e., tissue stoichiometry) across each species pair. Closed circles represent contrasts between species occupying different phylogenetic tribes while open circles represent contrasts between species occupying the same phylogenetic tribe. (C) Relationship of species-specific growth rates (from Haag and Rypel 2011) and tissue %P (mean ± SE). (D) Tissue N:P (mean ± SE) predicts excretion N:P (mean ± SE) of the unionid mussels in our study. The data shown here are for individuals with paired measurements tissue stoichiometry and excretion measurements (N=160). The four dominant phylogenetic tribes in our study area were Amblemini (blue diamond), Lampsilini (green circles), Pleurobemini (orange triangles) and Quadrulini (black squares).

Fig 4. Tanglegram comparing topologies based on molecular phylogenetic relationships and functional trait distances of molar stoichiometric ratios. Phylogenetic tribe is indicated by text color: Amblemini (blue), Lampsilini (green), Pleurobemini (orange) and Quadrulini (black). Parallel links

ending in the same tribes on both sides suggest conservatism. Divergence is indicated if phylogenetically closely related species are linked to different functional traits, whereas convergence may be occurring if phylogenetically unrelated species are pooled similarly by function.

Fig. 5. (A) Species richness and phylogenetic diversity were positively related across the seven communities. (B) The correlation between total species richness and functional dispersion across the seven sampled communities was best described with a unimodal relationship. (C) Shannon diversity had a negative relationship with functional dispersion across the communities. (D) The relationship between phylogenetic diversity and functional dispersion was best described by a unimodal relationship across communities.

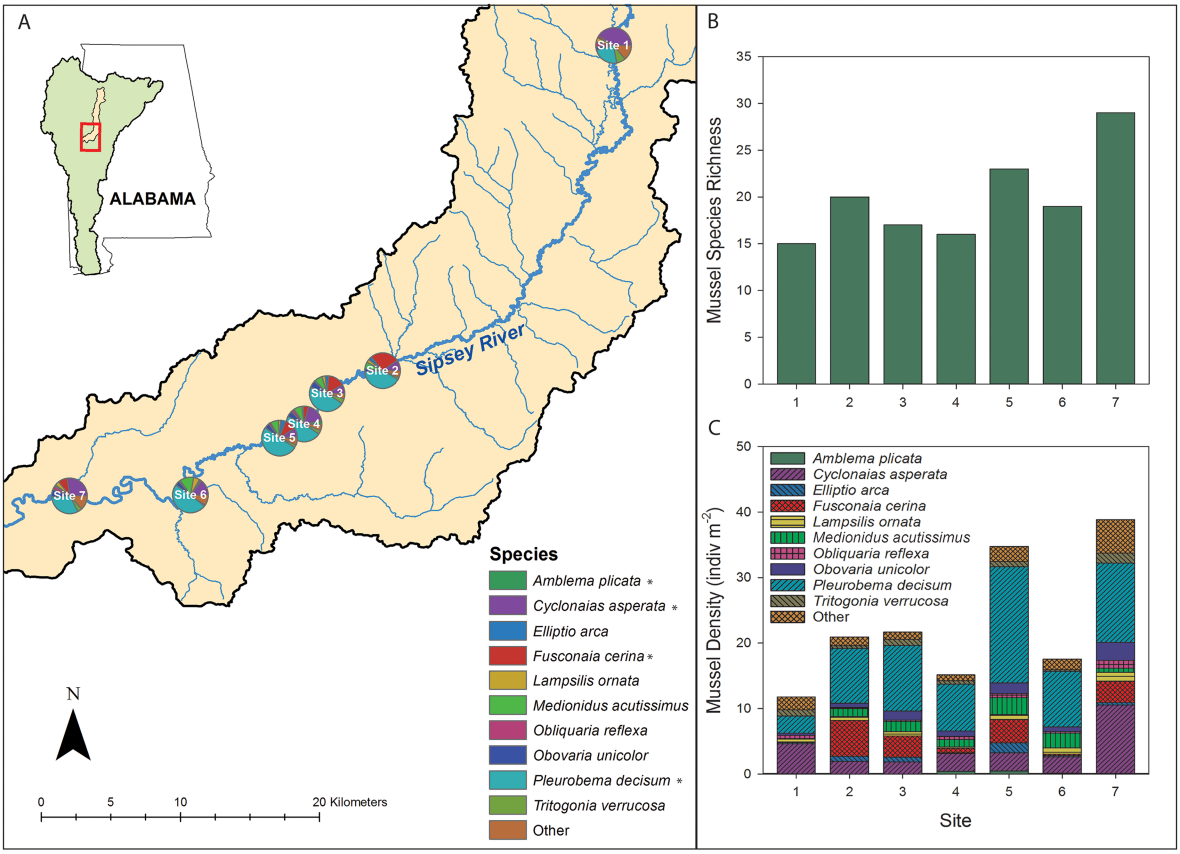

ecy_3100_f1.tif

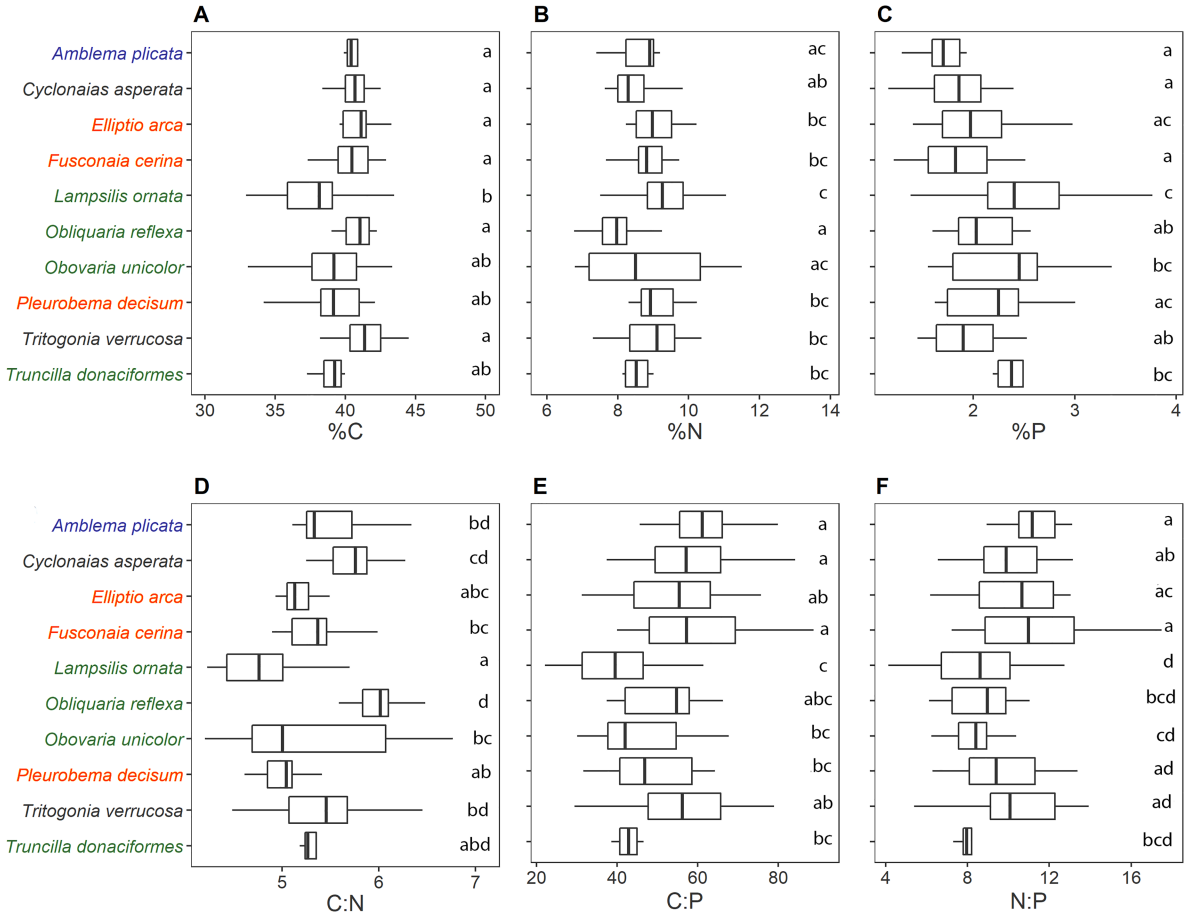

ecy_3100_f2.tif

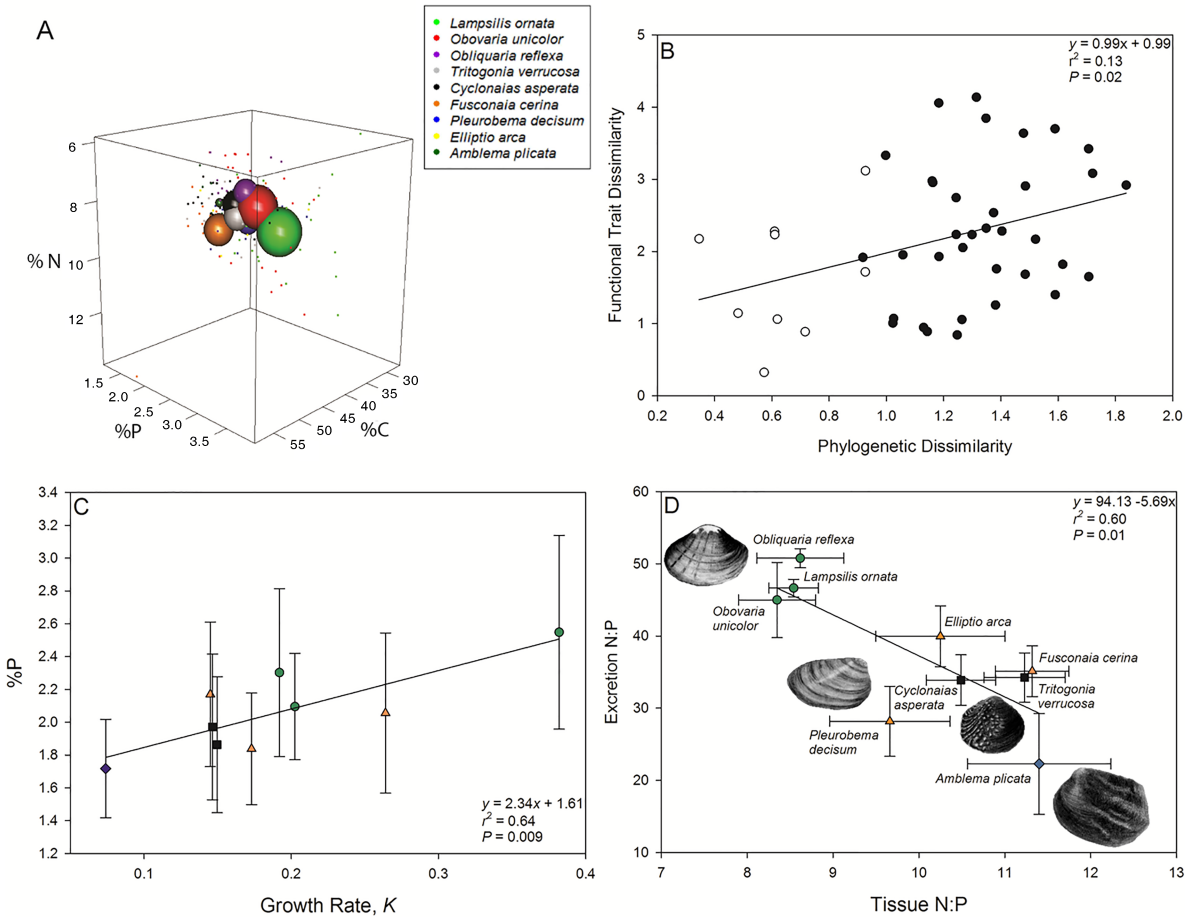

ecy_3100_f3.tif

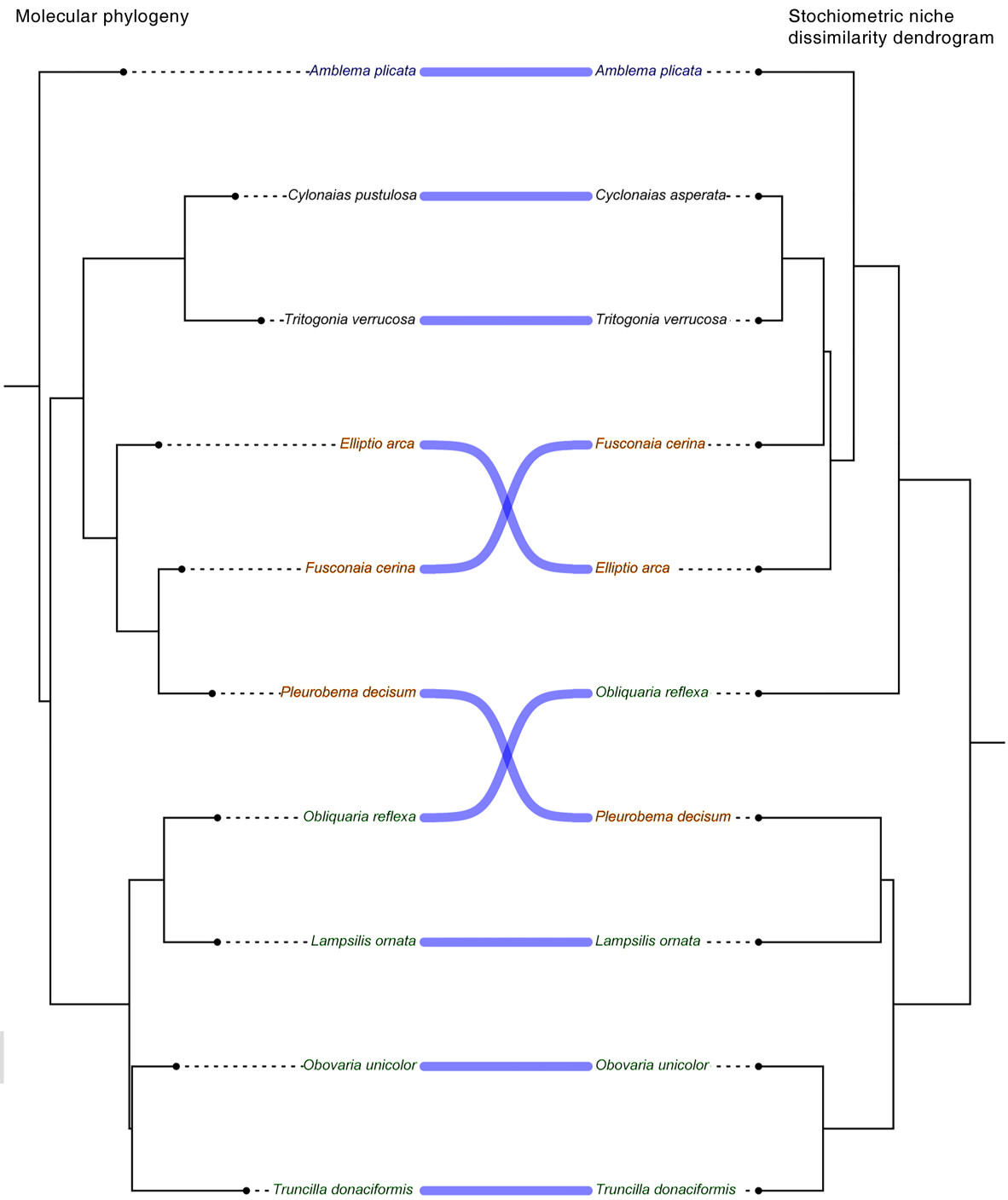

ecy_3100_f4.tif

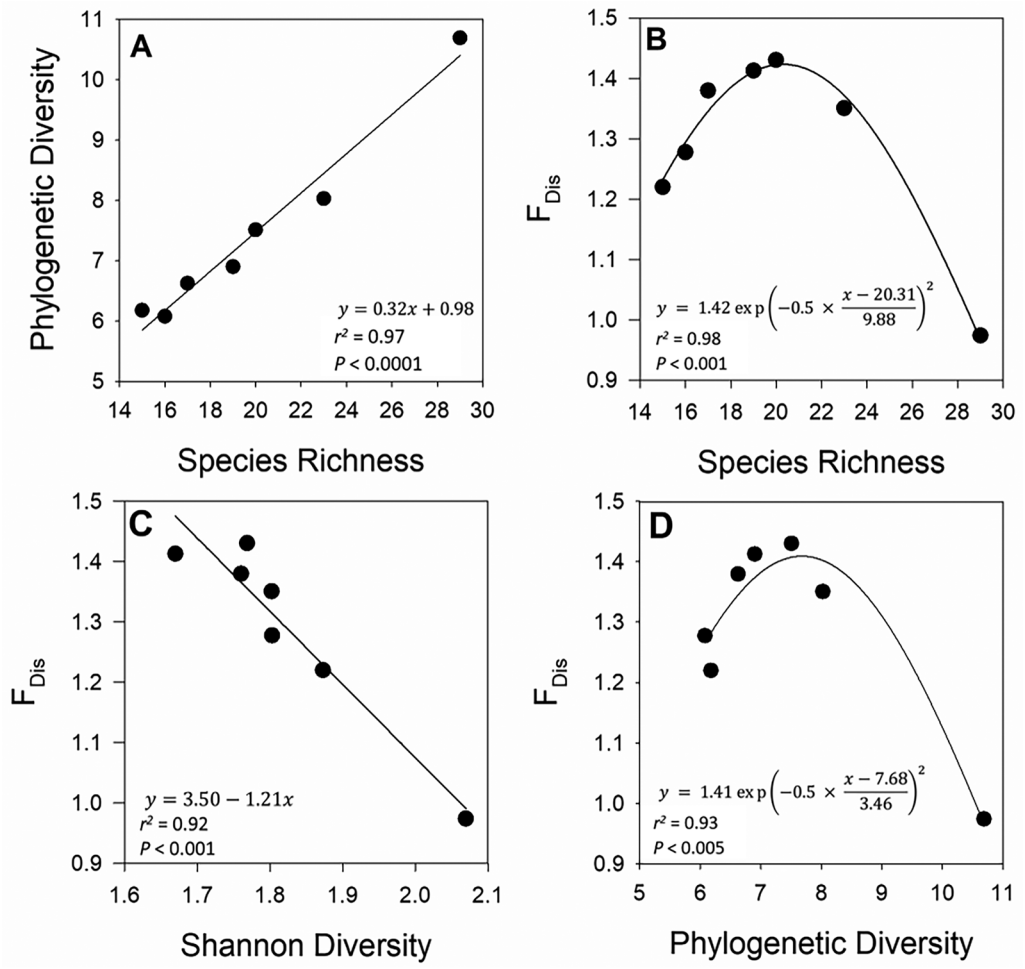

ecy_3100_f5.tif